SOLAR STORMS AND TOPOLOGY: OBSERVED WITH SDO

Henrik Lundstedt
Swedish Institute of Space Physics (IRF) Sweden[1]

Keywords
Solar storms, SDO, helicity, topology, linking number, braids, winding number

Abstract
From discussions with power industry we have learned that forecasts and warnings of the real strong solar storms and herewith large geomagnetic dB/dt nT/min are what would be of interest to them. The challenge for us is therefore to find the patterns when these strong solar storms occur: On long-term, topological studies of dynamo models will be described. On short-term, topological studies of real-time observations of Solar Dynamics Observatory (SDO) vectormagnetograms will be described. In these work I will apply the most recent research and also show some real-world events based on observed SDO data. I will also discuss historical events in the light of the most recent and advanced solar research.

Introduction

Today's very high-tech society has become very susceptible to strong solar storms, such as coronal mass ejections (CMEs) and solar flares. Fast Earth-directed CMEs may cause severe geomagnetic storms with large dB/dt variations and accompanied problems for the power industry [16]. Intense solar flares may cause problems to HF communications and aviation. World-wide forecast services of solar storms and space weather effects exist through fourteen Regional Warning Centers within the International Space Environment Service (ISES). Forecasts are based on space- and ground-based observations. However the latest research and observations show that we lack the necessary knowledge to forecast and understand the really severe solar storms and herewith a possible severe geoeffect. Historical records and astronomical observations of solar-type stars also tell us that we can be exposed to much stronger solar storms in future. Thousand times stronger flares on solar-like stars have been observed [19]. Agencies around the world have now started to work together in order to prepare for severe space weather effects [15]. Understanding severe solar storms is an important scientific challenge. In this article I will describe attempts, based on using the topology of the solar magnetic field [18]. A solar storms will be considered as a reduction of the magnetic field complexity. A measure of the complexity is the helicity, which can be interpreted topologically by the linking of magnetic flux tubes and field lines. Moderate solar storms observed with SDO will be compared to severe historical storms.

Topology of a Magnetic Field

Johann Benedikt Listing, student of Carl Friedrich Gauss, coined the word "Topology" in his essay 1847 "Vorstudien zur Topologie". Gauss defined (1833) [11] a linking number for two loops in $\mathbb{R}^3$. Loops i and j are described by two three-vectors $\bar{x}_i(s)$ and $\bar{x}_j(s)$. The Gauss linking number is defined as the integral

[1] IRF-Scheelevägen 17, 223 70, Lund

$$\mathcal{L}_{i,j} = \frac{1}{4\pi} \oint \oint \frac{(\bar{x}_i - \bar{x}_j)\cdot(d\bar{x}_i \times d\bar{x}_j)}{|\bar{x}_i - \bar{x}_j|^3} \quad (1)$$

Gauss showed that this integral is an integer and is invariant, as the loops i and j are deformed as long as they do not intersect each other.

The topology of a magnetic field at any instant of time refers to how field lines wind and braid each other. Magnetic helicity H (Hopf invariant [1]) for a closed region measures the average linkage of field lines

$$H = \int \bar{A} \cdot \bar{B}\, d^3x\,,\ \bar{B} = \nabla \times \bar{A}. \quad (2)$$

The Biot-Savart formula transforms the helicity integral to a dubbel integral

$$H = -\frac{1}{4\pi} \iint \bar{B}\,(\bar{x}) \cdot \frac{(\bar{x} - \bar{x}')}{|\bar{x} - \bar{x}'|^3} \times \bar{B}(\bar{x}')d^3x d^3x'. \quad (3)$$

This double integral clearly shows its origins in the Gauss linking number (eq 1.).

To describe the helicity for an open region, including a surface that helicity passes, we calculate the relative helicity [1] by decomposing the open field into a vacuum or potential field $\bar{P}$ plus a closed field. Applied to the corona it becomes

$$H_{corona} = \int_{corona} (\bar{A} + \bar{A}_p) \cdot (\bar{B} - \bar{P}) d^3x \quad (4)$$

where $\bar{A}$, $\bar{A}_p$ are the vector potentials.
The flow of helicity through the photosphere can now be deduced [4] as

$$\frac{dH_{corona}}{dt} = 2 \oint_{photosphere} ((\bar{A}_P \cdot \bar{B}_t)\, \bar{v}_n - (\bar{A}_P \cdot \bar{v}_t)\, B_n)\, d^2x \quad (5)$$

where $\bar{B}_t$, $\bar{v}_t$ represent the tangential magnetic field and the plasma velocity and B_n , v_n the normal to surface. The first term in eq (5) is associated with the magnetic flux emergence, whereas the second is associated with shearing/twisting motions. Introducing a velocity $\bar{u} = \bar{v}_t - \frac{v_n}{B_n}\bar{B}_t$ the photospheric helicity rate is simplified to

$$\frac{dH_{corona}}{dt} = -2 \oint_{photosphere} (\bar{A}_p \cdot \bar{u}) B_n d^2x \quad (6)$$

After $\bar{A}_p$ has been written in terms of the magnetic field helicity rate can be calculated directly from a time series of observed longitudinal magnetograms, where $\frac{d\theta_{ij}}{dt}$ is the roatation rate

$$\frac{dH_{corona}}{dt} = \sum_{i=1}^{N} \sum_{j=1}^{N} \frac{d\theta_{ij}}{dt}\, \phi_i \phi_j. \quad (7)$$

If we divide the magnetic field into N flux tubes of fluxes Φ crossing the boundary, then an expression for helicity of a general magnetic field configuration is given [10] by

$$H_m = \sum_{i=1}^{N} T_i\, \Phi_i^2 + \sum_{i=1}^{N} \sum_{j=1, j\neq i}^{N} \mathcal{L}_{i,j}\, \Phi_i \Phi_j \quad (8)$$

where the first term describes the self helicity and the second the mutual helicity. The Calugarreanu-White linking number T_i is the sum of the writhe (Wr) and the twist (Tw). For closed magnetic flux tubes $\mathcal{L}_{i,j}$ is the Gauss linking number. In [10] Demoulin et al. show how to

calculate $\mathcal{L}$ for two loops a and c (Fig 1).

$$\mathcal{L}_{a,c} = \frac{1}{2\pi}(\theta^m_{c+a-} - \theta^m_{c+a+} + \theta^m_{c-a+} - \theta^m_{c-a-}) \quad (9)$$

The multi-valued function θ^m keeps track of how much foot points $c_\pm$ are rotating around foot points $a_\pm$, taking into account both translational and rotational motions. The important thing with this metods is that the helicity can be calculated based on direct observations and on longitudinal photospheric magnetic field measurements. The helicity is also succesively built up and the connectivity of the field lines is included.

Figure 1: Two linked flux tubes a, c of braided magnetic field lines.

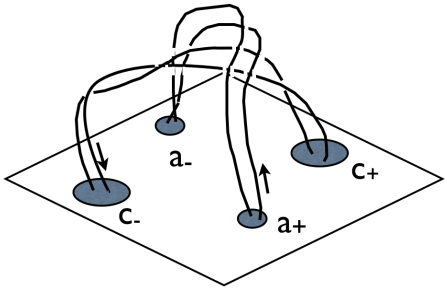

Just as with the Gauss linking number, magnetic helicity is the lowest order of topological measure. The Gauss linking integral and herewith helicity fails e.g. to detect the entanglements of curves in R^3 with an equal number of oppositely signed crossings. Berger [5] therefore introduced a second order winding number invariant in order to describe the linking of three braided curves and not just two as for helicity. The braiding is projected to a complex plane where the winding is described by the winding integral. More complex braided patterns can then be studied and herewith more severe solar storms.

The Dynamo and Coronal Solar Storms

In [27] Warnecke et al. show that a helicity driven turbulent dynamo produces CME-like plasma ejections. In so-called Stretch Twist Fold (STF)-dynamos [7], the chaotic plasma motions below the solar surface produce strong twisted magnetic flux tubes that emerge through the surface. In Fig. 2 we illustrate a simple model of STF. A torus flux tube is described by,

$$\{(\phi, w) \in C \times B : 0 \leq \phi < 2\pi, |w| \leq 1\} \quad (10)$$

We then stretch and fold it by iteration of the function

$$f(\phi, w) = (2\phi(mod\ 2\pi), aw + \tfrac{1}{2}\hat{\phi}) \quad (11)$$

($0 < a < ¼$) and twisted strands of different sizes are now seen in Fig. 1. The fractal dimension is given by

$$s = 1 + \log 2 / -\log a \quad (12)$$

Figure 2: A stretched, twisted and folded model. An active region observed by HMI on board SDO and corresponding multifractal spectra.

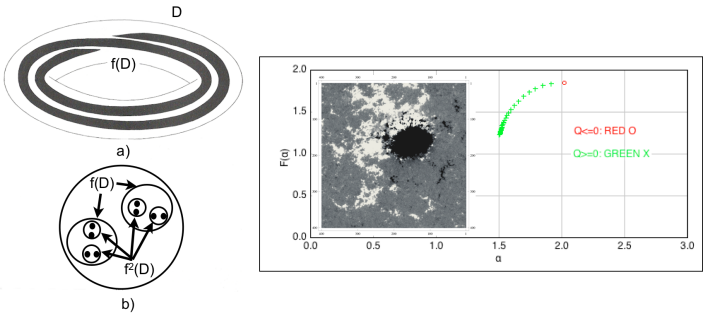

The model suggests we would observe a multifractal magnetic field. Using a LOS magnetogram (HMI/SDO) of AR 1131 Decemeber 7, 2010 we measured just that and a multifractal spectra (Fig. 2) with a maximum value for F(α) of 1.8592. The chaotic motions herewith produce a multifractal and also braided, twisted emerging flux through the photosphere.

Berger [3] estimated that the free energy, stored in the braided field, is proportional to the square of the crossing number C_{min}. Φ stands for the magnetic flux of the flux tubes, N the number of strands of the braid (=flux tubes) and L the length.

$$E_m \geq 9.06 \times 10^{-2} \, (C_{min})^2 \, \frac{\Phi^2}{N^2 L} \qquad (14)$$

Interestingly it is also found [6] that the solar flare energy released due to reconnection of the braids in the coronal loops follows a power-law distribution, i.e. is fractal.

In a study of a complex generalization of a Lorenz-type dynamo [16] we found that the flow had an attractor and fractal structure. We have also found in a follow-up study that grand cycle maxima are clustered. Severe solar storms might therefore also come in clusters. The dynamo and motion of photospheric flux tubes produce magnetic helicity which are accumulated in the corona [10]. The conservation of helcity therefore requires it to be reduced. Coronal solar storms (solar flares [2] and CMEs [28]) might be the way. The found dynamo clustering of times of severe solar activity makes one speculate that even severe solar storms are clustered on long-terms. This is something we will further study.

Moderate Solar Storms Observed with SDO

Let us now start with a description of some moderate solar storms observed by SDO. Since SDO's launch, 11 February 2010, the Sun has produced 17 proton events and 14 halo CMEs.

Figure 3: Observation of solar storm on 30 March, 2010 with HMI/AIA instruments onboard SDO and LASCO C2 onboard SOHO.

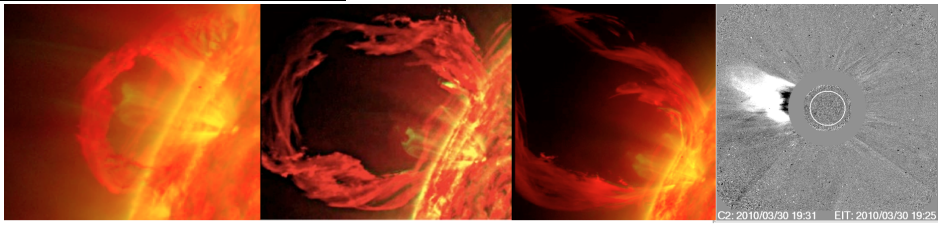

Erupting prominence, 30 March, 18.08 UT, SODO, AIA.

Erupting prominence, 30 March, 18.32 UT, SODO, AIA.

Erupting prominence, 30 March, 18.48 UT, SODO, AIA.

CME, 30 March, 19.25 UT, SOHO, C2.

Fig. 3 shows an eruption of a prominence on 30 March 2010. The first three images were observed with the AIA instrumnet onboard SDO in wavelengths 1800 Å, 304 Å and 171 Å and the last with the C2 coronagraph instrument onboard SOHO. In the second sharpened image we can clearly see that the prominence consisted of many twisted flux ropes of many different sizes. In the third image the rotation has stopped, broken up probably due to a kink instability [26] and plasma also started to fall down. Finally, in the forth image SOHO is observing a CME leaving the Sun [15].

The first observed X class solar flare on the new solar cycle 24 occurred on February 15, 2011. Solar flares are classified by X-ray peak burst intensity I in 0.1- 0.8 nm and Wm^{-2} (M class flares $1.0 \cdot 10^{-5} \leq I \leq 1.0 \cdot 10^{-5}$ and X class flares $I \geq 1.0 \cdot 10^{-4}$). The AR 1158 produced an X2.2 X-ray solar flare on Feb 15. The magnetic region was described as β–γ–δ complex and having a size of about 785 millions (i.e. bipolar but so complex that no continuous line can be drawn between spots of opposite polarity (β–γ), and also having one or more sunspot umbra separated by less than 2° within one penumbra of opposite polarity (δ)). A halo CME occurred. No proton event was reported. The vector field, observed by HMI/SDO [24] showed both a rotation, twist and a stretching of the field at time of the solar flare.

Figure 4: Observation of solar storm on 15 February, 2011 with HMI/AIA instruments onboard SDO and STEREO.

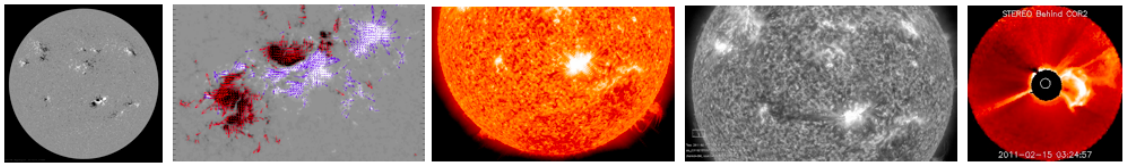

[13] found that the helicity was reduced after the major flares of the AR 1158. Interestingly the flare also triggered other activity far from the flare location. A so called global solar storm took place [21], [22]. Transporting of helicity between active regions has therefore also become interesting.

The next event took place in January 2012 and a release of magnetic energy stored by twisting.

Figure 5: Observation of solar storm on 27 January, 2012 with HMI/AIA instruments onboard SDO and LASCO C2 onboard SOHO.

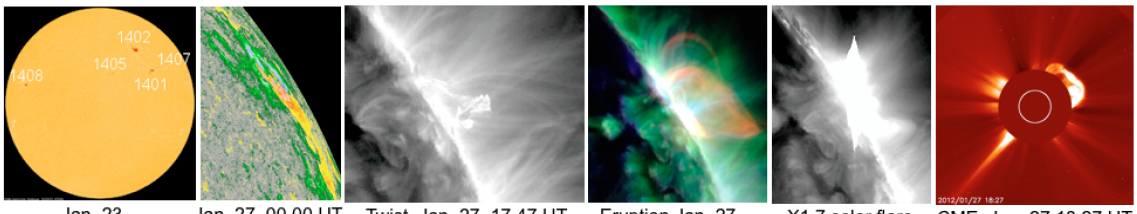

During the late January 2012 event we could follow the winding of the coronal loop, appearance of a kink instability, followed by CMEs and solar flares. Small flux changes appeared and the magnetic complexity reached β–γ. The AR reached a size of at 500 millions. On 23 January AR

1402 produced an M8 X-ray flare, a halo CME and a proton event of 6310 pfu. On 27 January an X 1.7 solar flare, a halo CME and a proton event of 796 pfu (particle flux unit = pfu, 1 p cm^{-2} s^{-1} sr^{-1}).

The last solar storm observed with SDO that we will describe took place in July 2012. The AR 1520 of July 2012 reached a β–γ–δ complexity. The region grew to an impressive size of 1460 millions. An intrusion of negative polarity flux occurred in the positive umbra of the spot at 13 UT on 12 July and disappeared on 14 July 1 at 09 UT. An X 1.4 solar flare and a halo CME occurred that produced a proton event of about 100 fpu. An interesting coronal S-shaped sigmoid structure occurred just before the solar flare. One may therefore suspect a kink instability again occurred as in January 2012 event. The active region 1520 continued to produce CMEs on the far side. On 23 July a very fast CME 2930 km/s was reported by NASA Space Weather Laboratory.

Figure 6: Observation of solar storm on July 12, 2012 with HMI/AIA instruments onboard SDO and LASCO C2 onboard SOHO.

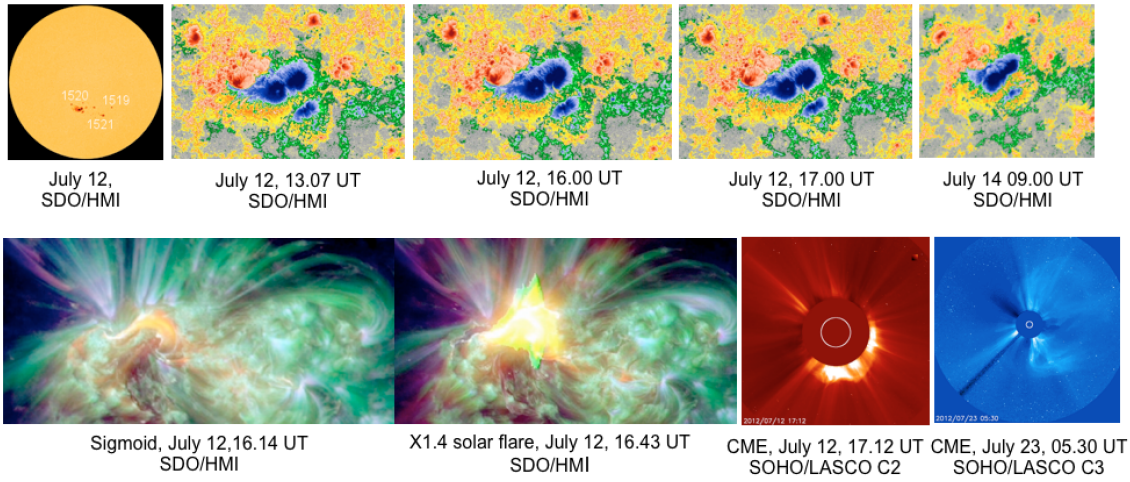

The possibility of SDO to observe the whole Sun all the time has clearly emphasized the importance of topology and particularly the helicity for understanding occurrence of solar storms.

Severe Solar Storms Observed in May 1921 and in October 2003

The first white-light (type II) solar flare was observed on 1-2 September 1859, during the Carrington event. The first CME was observed 14 July, 1860 during solar eclipse, i.e. in visual light. In 1908 George Hale at Mount Wilson (MW) was able to measure the solar magnetic field using the Zeeman effect. That led to a breakthrough in the search for a pattern behind solar activity. During the super solar storm 12-16 May 1921 (Fig. 7 and 8) [20], [25] we therefore could also study the complexity of the solar magnetic field at the solar flare and presumably CME, together with the visual observations from several observatories. The active region 1842 showed magnetic complexity (β–γ) and was located near the center at low latitude. The spot group, Greenwich number 9334, had a mean area of 1324 millionths of the Sun's visible hemisphere, i.e. large but not the largest observed. An area as large as 6132 was e.g. measured for AR on 8 April 1947. The AR 486 of the Halloween event 2003 reached for example 2600 millions. The size is therefore not of prime importance. The region 9934 with three large sunspots showed flux changes especially on 12 May. On 13 and 14 May also disappearing and emerging of new flux occurred. We also notice a rotation of both sunspot groups, from being

parallel to equator to perpendicular. Very strong magnetic flux density between +3.4 kG and –3.5kG was measured by MW. We expect a reduction of helicity caused the severe solar storms. The solar storms 9334 occurred as for the Carrington events during mediocre sunspot cycle and during the declining phase of cycle 15. Geomagnetic activity occurred mainly at about 20 GMT on 13 May , 21-24 UT on 14 May and 04-06 UT on 15 May. The first sudden commencement (S.C.) occurred at 13 GMT on 13 May [8]. We assume at least three CMEs left the Sun. Probably as many as four since four sudden commencements were observed [RGO]. Very interestingly, a value dB_h/dt as high as about 5000nT/min has been estimated for 14 May [14]. Aurora as close to magnetic equator as Samoa has been observed [23]. That makes the 1921 event to one of the strongest space weather events ever reported.

Figure 7: Active region 1842 observed 12-16 May 1921, at Mount Wilson Observatory and at Royal Greenwich Observatory.

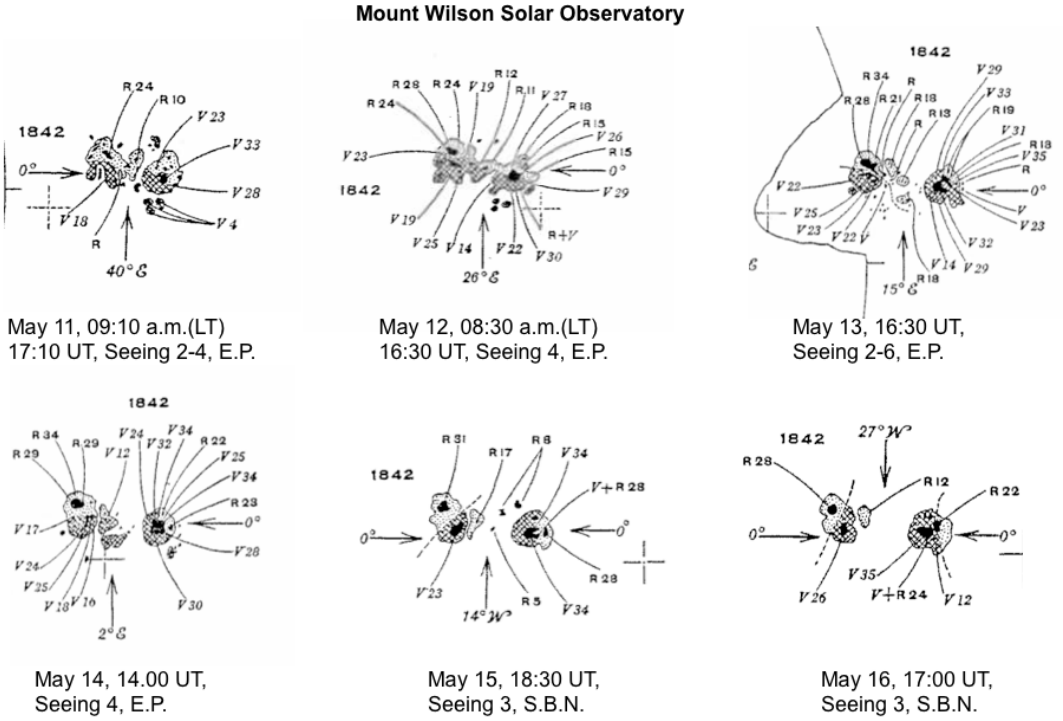

Figure 8: The same active region observed from Royal Greenwich Observatory (RGO), both from UK and Cape. On 15 May we show observations from Kvistaberg in Sweden instead due to bad seeing at RGO.

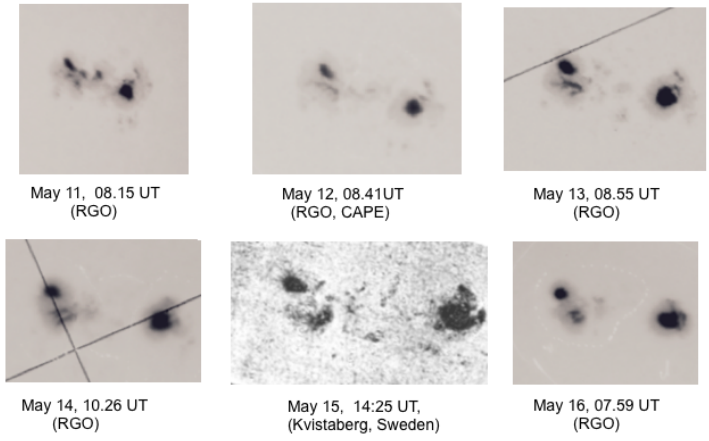

Let us now finish with the most recent severe solar storms that took place in 2003, during the Halloween events in solar cycle 23. The AR 486 produced on 28 October an X17 X-ray solar flare, and full halo CMEs with an estimated speed of 2125km/s with proton flux of 29 500 pfu, on 29 October an X10 , and another halo CME on the 29 with a speed of 1948 km/s (transit time 19hrs). The magnetic field ranged between +2.6 and -2.6 kG. The magnetic complexity reached β−γ−δ. Large flux changes and a strong kinetic helicity were observed [12] (Fig. 10). The size of AR 486 was estimated to about 2600 millions.

Figure 9: Observation of the Halloween solar storms with the MDI instrument onboard SOHO (mirrored) and corresponding Mount Wilson drawings.

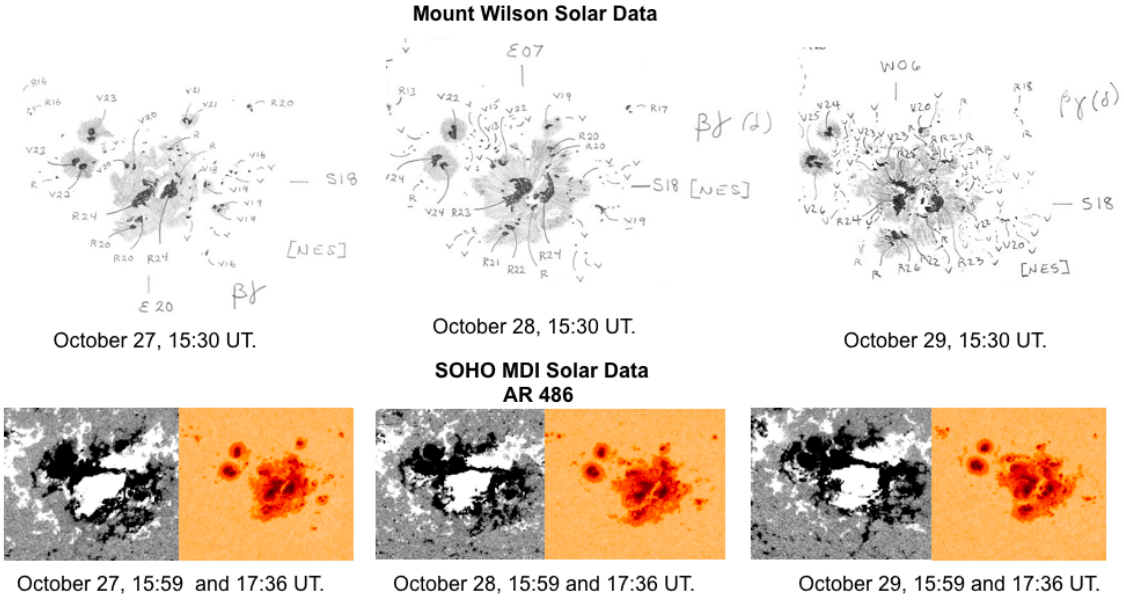

Figure 10: Observation of the Halloween solar storms with the MDI instrument onboard SOHO and strong downflows (yellow) at the AR 486 with associated strong magnetic fields and solar flares (black dots).

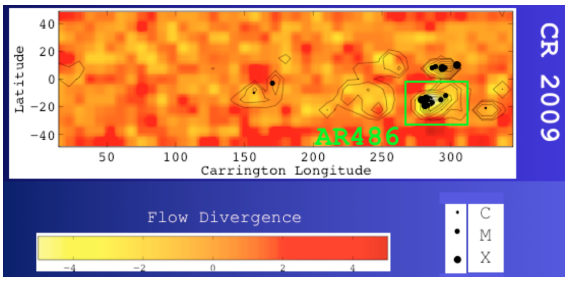

Fig. 10 shows the strong downflows (kinetic helicity) in AR 486 and herewith high magnetic helicity that was reduced in association with the strong solar flares during the Halloween event.

Summary and Discussion

The topology of the solar magnetic field describes the complexity and herewith the energy possibly to be released in a solar storm. A key factor is the braiding within and among the fluxtubes. The braiding may have already been produced by a dynamo below the solar surface or by the rotation and fragmentation of the flux tubes on the surface. In this article we suggest the

braiding and its reduction as well as the helicity as the cause of solar storms. We have given both recent examples, observed with SDO, STEREO and SOHO, and historical ones.

Figure 11: Solar storms of 1921 May, 2003 October and 2012 in July/August .

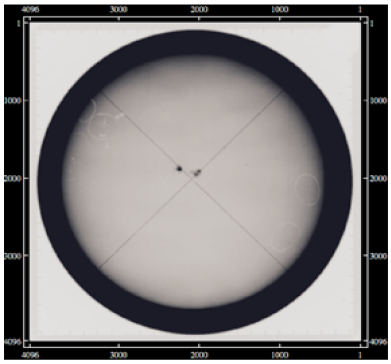

AR 9334 Greenwich number, May 14, 10.25 GMT, 1921, RGO.

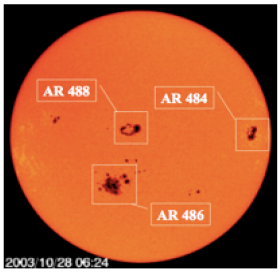

AR NOAA 488, 486, 484, October 28, 06.24 UT 2003, SOHO/MDI.

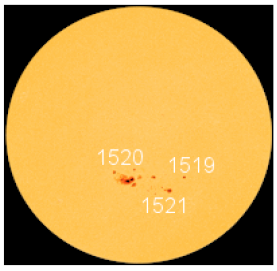

AR NOAA 1520, 1519, 1521, July 14, 2012, SDO/HMI.

How was the 1921 event compared to the Carrington event 1859, from a solar point of view? Did the 1921 event also produce proton events and white-light solar flares? Cliver et al. [9] cannot find any evidence for that. However, lack of observations does not preclude that it occurred. If we compare the drawings by Mt Wilson of May 1921 with the Halloween event on 27-29 October, 2003, which one should we have expected to produce the strongest solar storms? In favour of the 1921 event we notice in Fig. 7 a stronger magnetic field in AR 1842 in AR 486 of 2003 as measured by MW.

How different were the events that took place in May 1921, October 2003 and July 2012? What was the key factor that made the solar storm of 1921 a severe solar storm, the magnetic field strength? From the observations we have seen that the strength of the magnetic field, the rotation, twist, the braiding, not so much the size of the active region played an important role for the severity of the solar storms.

Acknowledgements

I thank T. Hoeksema and the SDO HMI solar team at Stanford, SDO AIA team at Lockheed, the SOHO team, Mount Wilson Observatory, S. Matthews, Univ. College London, Dept. of Space & Climate Phys. Solar & Stelllar Phys. Group, Mullard Space Science Laboratory for RGO 1921 and NOAA SWPC for the data used.

References

[1] Arnold, V. I. And B. A. Khesin, (1998). Topological Methods in Hydrodynamics, Applied Mathematical Sciences 125, eds. J.E. Marsden and L. Sirovich. Springer Verlag.

[2] Benz, A. O. (2008). Flare Observations. Living Rev. Solar Phys., Vol. 5, pp. 1-64. Max Planck Society.

[3] Berger, M. (1993). Energy-Crossing Number Relations for Braided Magnetic Fields. Phys. Rev. Lett., Vol. 70. 6., pp- 705-708. American Phys. Society.

[4] Berger, M. (1999). Magnetic Helicity in Space Physics in Magnetic Helicity in Space and Laboratory Plasma. Efditors M. R. Brown, R. C. Canfield and A. A. Pevtsov. AGU Geophys

Monograph 111.

[5] Berger, M. (2009) . Topological Quantities: Calculating Winding, Writhing, Linking, and Higher order Invariants. Lectures on Topological Fluid mechanics. Editor: R. L. Ricca. Springer Verlag.

[6] Berger, M. (2009). Self-Organized Braiding and the Structure of Coronal Loops. Astrophys. J., 705. pp. 347-355. AAS.

[7] Childress, S. and A.D Gilbert (1995) Stretch, Twist, Fold: The Fast Dynamo, Springer Verlag.

[8] Chree, C. (1921). The Magnetic Storm of May 13-17. Nature Vol. 107. pp.359-359. Nature Publ. Group.

[9] Cliver, E. W. and L. Svalgaard. (2004). The 1859 Solar-Terrestrial Disturbance and the Current Limits of Extreme Space Weather Activity, Solar Phys. Vol. 224, pp. 407-422. Springer.

[10] Demoulin, P., E. Pariat, and M. A. Berger. (2006). Basic Properties of Mutual Helicity. Solar Phys., Vol. 233. pp. 3-27. Springer.

[11] Epple, M. (1999). Geometric aspects in the development of knot theory, pp 301-357. in History of Topology, edited I. M. James, Elsevier Science B. V..

[12] Jensen, J. M., Lundstedt, H., Thompson, M. J., Pijpers, F. P., and Rajaguru, S. P. (2004). Application of Local-Area Helioseismic Methods as Predictors of Space Weather, in Helio- and Asteroseismology: Towards a Golden Future, ed. D. Danesy, Proc. SOHO 14/GONG+ 2004 Meeting, ESA SP-559, 497-500, 2004.

[13] Jing, J., Park, S-H., Liu, C., Lee, J., Wiegelmann, T., Xu, Y., Deng, N. and H. Wang. (2012). Evolution of Relative Helicity and Current Helicity in NOAA Active Region 11158. Astrophys. J. Lett., 752:L 9. 7pp. AAS.

[14] Kappenman, J. G. (2006). Great geomagnetic storms and extreme impulsive geomagnetic field disturbance events – An analysis of observational evidence including the great storm of May 1921. Adv. Space Res., Vol. 38. pp. 188-199.

[15] Koleva, K., Madjarska, M. S., Duchlev, P., Schrijver, C. J., Vial, J. –C., Buchlin, E., and M. Dechev. (2012). Kinectics and helicity evolution of a loop-like eruptive prominence. Astron. and Astrophys., pp9. ESO 2012.

[16] Lundstedt, H. (2006). The Sun, space weather and GIC effects in Sweden. Adv. Space Res.,. Vol. 37. pp. 1182-1191. Elsevier Ltd.

[17] Lundstedt, H. and T. Persson, (2010). Modelling solar cycle length based on Poncaré maps for Lorenz-type equations. Ann. Geophys. Vol. 28. pp. 993-1002. Copernicus Publications.

[18] Lundstedt, H. (2010). Solar storms, cycles and topology. The European Physical Journal. Vol. 9. pp. 95-103. EDP Sciences.

[19] Maehara, H., T. Shibayama, S. Notsu, Y. Notsu, T. Nagao, S. Kusaba, S. Honda, D. Nogami, K. Shibata, (2012). Superflares on solar-type stars. Nature. Letter. Vol. 485. pp. 478-481.

[20] Royal Greenwich Observatory. (1955). Sunspot and Geomagnetic-Storm Data, derived from Grenwich observations, 1874-1954. Her Majesty's Stationary Office, London.

[21] Schrijver, C. J., Aulanier, G., Title, A. M., Pariat, E. and C. Delanné. (2011). Astroph. J., 697, 736, 102.

[22] Schrijver, C. J.and A. M. Title. (2011). Long-range magnetic coupling between solar flares and coronal mass ejections observed by SDO and STEREO. J. Geophys. Res., Vol. 116, A04108.AGU.

[23] Silverman, S. M., and E. W. Cliver. (2001). Low-latitude auroras: the magnetic storm of 14-15 May, 1921. J. Atmos. Solar-Terr., Phys., Vol. 63, pp. 523-535. Elsevier Science Ltd.

[24] Schou, J., Scherrer, P. H., Bush, R. I., et al. (2012). Solar Phys., 275, pp229.

[25] Tamm, N. (1922). Die grossen Sonneflecken Mitte Mai und Anfang Juni 1921. Astronomische Nachrichten. Vol. 216. p209.

[26] Török, T., M. A. Berger and B. Kliem. (2010). The writhe of helical structures in the corona. Astron. And Astrophys., p516, A49.

[27] Warnecke, J., A. Brandenburg, and D. Mitra. (2011). Dynamo-driven plasmoid ejections above a spherical surface. Astron. and Astrophys. Vol. 534. pp. 1-10. EDP Sciences.

[28] Webb, D. F. and T. A. Howard, (2012). Coronal Mass Ejections: Observations. Living Rev. Solar Phys., Vol. 9. pp. 3-81. Max Planck Society.

Biography

Henrik Lundstedt earned his Ph.D in Astronomy at Lund University on solar-terrestrial research carried out at Stanford University in California. He led a research project on producing magnetograms for the Swedish solar telescope on La Palma, Canary Islands and managed to obtain measurements of intergranular magnetic fields. He developed the first forecasts of geomagnetic activity, based on solar wind input ACE data, using neural networks. He has participated in ESA's space weather projects and consortiums from the beginning 1995. He has also participated in EU COST actions 720 and 0803. Lundstedt started the Regional Warning Center RWC-Sweden 2000 of the International Space Environment Service (ISES) and became Deputy Director ISES in 2004. Lundstedt particitpated in the NOAA/NASA Cycle 24 Prediction Panel 2008. He has arranged several workshops on AI Applications in Solar-Terrestrial Physics and Solar Magnetic Activity. He leads the research project "Solar storms and space weather" granted by the Swedish Civil Contingency Agency. A workshop is planned for 2014 on solar magnetic activity and topology. He has collaborated with the solar group at Stanford, since the 1980s, and now focuses on using vectormagnetograms observed with SDO to understand the solar magnetic activity topologically.